Hindawi
International Journal of Intelligent Systems
Volume 2023, Article ID 3028824, 15 pages
https://doi.org/10.1155/2023/3028824

Research Article

Modeling and Analysis of the Fuzzy-Fractional Chaotic Financial System Using the Extended He–Mohand Algorithm in a Fuzzy-Caputo Sense

Mubashir Qayyum[1] **Efaza Ahmad,**[1] **Aneeza Tahir,**[1] **and Saraswati Acharya**[2]

[1]*Department of Sciences and Humanities, National University of Computer and Emerging Sciences, Lahore, Pakistan*
[2]*Kathmandu University School of Science, Dhulikhel, Nepal*

Correspondence should be addressed to Saraswati Acharya; saraswati.acharya@ku.edu.np

Received 22 May 2023; Revised 20 October 2023; Accepted 24 October 2023; Published 4 November 2023

Academic Editor: Vasudevan Rajamohan

This paper contains modeling of a fuzzy-fractional financial chaotic model based on triangular fuzzy numbers (TFNs) to predict the idea that long-term dependency and uncertainty both have an impact on the financial market. For solution purposes, the He–Mohand algorithm is proposed where homotopy perturbation is hybrid with Mohand transform in a fuzzy-Caputo sense. In analysis, solutions and corresponding errors at upper and lower bounds are estimated. The obtained numerical results are displayed in tables to show the reliability and efficiency of the proposed methodology. Upper bound errors range from 10^{-6} to 10^{-12} and lower bound errors from 10^{-6} to 10^{-11}. For graphical analysis, system profiles are illustrated as two-dimensional and three-dimensional plots at diverse values of fractional parameters and time to comprehend the physical behavior of the proposed fuzzy-fractional model. These plots demonstrate that the interest rate, price index, and investment demand decrease with the increase of the value of the $\mathfrak{r}$-cut at the lower bound. At the upper bound, this behavior is totally opposite. The chaotic behavior of the system at smaller values of saving rate, elasticity of demands, and per-investment cost is greater in contrast to their larger value. Analysis reveals that the proposed methodology (He–Mohand algorithm) provides a new way of understanding the complicated structure of financial systems and provides new insights into the dynamics of financial markets. This algorithm has potential applications in risk management, portfolio optimization, and trading strategies.

1. Introduction

Financial modeling [1] is the process of building mathematical models to represent the performance of portfolios, financial assets, or businesses. Its aim is to provide a quantitative representation of the underlying financial conditions and to make predictions about future performance. Numerous uses for these models are possible, such as scenario analysis, valuation, planning, risk assessment, and forecasting. Several quantitative techniques are used in financial modeling. Monte Carlo simulation [2], statistical analysis [3], sensitivity analysis [4], discounted cash flow [5], time-series analysis [6], and regression analysis [7] are some of them. It also requires in-depth knowledge of accounting principles, economic theory, and financial markets. There are various categories of financial models such as option pricing models [8], discounted cash flow models [9], chaotic financial models [10], portfolio optimization models [11], and credit risk models [12]. Each model has strengths and shortcomings and the best model relies on the application at hand as well as the facts that are accessible.

A fuzzy differential equation (FDE) is a type of differential equation in which some of the initial conditions or parameters are represented by fuzzy sets [13]. In various situations, the values of these initial conditions or parameters are not known precisely, but rather within a particular range. With the use of fuzzy differential equations, we can simulate the uncertainty that arises from such circumstances. These equations have many applications in various fields, such as fluid dynamics [14], kinetics [15], finance [16], economics [17], and biology [18]. Fuzzy Volterra integrodifferential equations [19], fuzzy Fisher model [20], fuzzy population growth model [21], first-order linear fuzzy differential equations [22], and fuzzy singular integrodifferential models [23] are some examples of fuzzy differential equations.

Fuzzy differential equations are also modeled in fractional derivative form. An extension of a derivative to a noninteger order is known as a fractional derivative. It is described using fractional calculus [24], which is a field of mathematics that manages noninteger order integrals and derivatives. Many physical models including the Lotka–Volterra population equation [25], coupled Schrodinger system [26], Oldroyd 6-constant fluid [27], Grey system models [28], tumor models [29], and Wu–Zhang system [30] exploit a fractional derivative approach. We can model and examine real-world problems that include uncertainty and fractional order derivatives by utilizing fuzzy-fractional differential equations (FFDEs). Oceanography [31], biological population model [32], COVID-19 model [33], heat equation [34], and Fisher's equation [35] are some areas that employ FFDEs. The Caputo fractional derivative [36] is one of the more popular definitions of the fractional derivative. It is commonly used in physics and engineering. It is described as a modification of the Riemann–Liouville derivative [37] that prevents the singular behavior at the lower limit of the integral. The Caputo fractional derivative is especially beneficial in modeling systems with memory or hereditary properties, such as Brinkman-type fluid [38], Korteweg–de Vries system [39], mosaic disease model [40], relaxation-oscillation equations [41], plant disease model [42], Casson nanofluid model [43], and chaotic system [44].

Due to the nonlocality of fractional derivatives as well as the complexity of fuzzy sets, solving FFDEs can be challenging. In literature, several techniques have been utilized to solve them. Rexma Sherine et al. [45] used the fuzzy-fractional Laplace transform method to estimate the spread of the generalized monkeypox virus model. The fractional differential transform method and Hilbert space method were combined by Najafi and Allahviranloo [46] to solve fuzzy impulsive fractional differential equations. The Legendre spectral method to find the solution of the fuzzy-fractional coronavirus model is adopted by Alderremy et al. [47]. To examine fuzzy-fractional differential equations, Alijani et al. [48] applied Spline collocation methods. Alaroud et al. [49] employed an analytical numerical technique on fuzzy-fractional Volterra integrodifferential equations. The Chebyshev spectral method was utilized by Kumar et al. [50] to analyze the fuzzy-fractional Fredholm–Volterra integrodifferential equation. A powerful tool to solve nonlinear fractional differential equations in fuzzy form is the He–Mohand method [51]. It is an efficient technique that provides a practical method for solving differential models by combining the homotopy perturbation technique (HPM) and the Mohand transform. Thus, in order to solve the fuzzy-fractional chaotic financial system, we have created an extended HPM hybrid using the Mohand transform.

The format of this article is as follows. In Section 2, preliminaries are given in which Mohand transform, Caputo fractional derivative, and its Mohand transform, fuzzy sets, and triangular fuzzy sets are defined. Section 3 is focused on the modeling of the fuzzy-fractional financial chaotic model. The solution framework based on the He–Mohand algorithm is presented in Section 4, whereas, the theoretical analysis of the proposed scheme is presented in Section 5. The focus of Section 6 is on the application and solution of the given system. Results of the study are discussed in Section 7 and, Section 8 provides some important conclusions of the study.

2. Preliminaries

Definition 1. [52]

The Mohand transform $\mathscr{M}$ of the function $\widetilde{\mathscr{G}}(\tau)$ for $\tau \geq 0$ is given by the following equation:

$$\mathscr{M}\left\{\widetilde{\mathscr{G}}(\tau)\right\} = \mathscr{K}(\tau) = p^2 \int_0^\infty \widetilde{\mathscr{G}}(\tau) e^{-p\tau} \mathrm{d}\tau, \quad p \in [k_1, k_2], \tag{1}$$

where $k_1, k_2 > 0$ can be finite or infinite. The parameter p factors the variable τ in the argument of function $\widetilde{\mathscr{G}}$.

Definition 2. The inverse Mohand transform $\mathscr{M}^{-1}$ of the function $\mathscr{K}(\tau)$ 1 is as follows:

$$\mathscr{M}^{-1}\{\mathscr{K}(\tau)\} = \frac{1}{2\pi\imath} \int_{\gamma-\imath\infty}^{\gamma+\imath\infty} \frac{1}{p^2} \mathscr{K}(\tau) e^{p\tau} \mathrm{d}p, \quad p \in [k_1, k_2]. \tag{2}$$

Definition 3. [53]

For a function $\widetilde{\mathscr{G}}(\tau)$, the Caputo fractional derivative ${}^C\mathbb{D}_\tau^\gamma$ is defined as follows:

$${}^C\mathbb{D}_\tau^\gamma\left\{\widetilde{\mathscr{G}}(\tau)\right\} = \frac{1}{\Gamma(\varepsilon-\gamma)} \int_0^\tau (\tau - P)^{\varepsilon-\gamma-1} \widetilde{\mathscr{G}}^{(\varepsilon)}(P) \mathrm{d}P, \quad \varepsilon - 1 < \gamma \leq \varepsilon. \tag{3}$$

Definition 4. [54]

The Mohand transform $\mathscr{M}$ in the presence of Caputo fractional derivative (3) can be written as follows:

$$\mathscr{M}\left\{{}^C\mathbb{D}_t^\gamma \widetilde{\mathscr{G}}(\tau)\right\} = p^\gamma \mathscr{M}\left\{\widetilde{\mathscr{G}}(\tau)\right\} - \sum_{a=0}^{\varepsilon-1} p^{\gamma-a+1} \widetilde{\mathscr{G}}^{(a)}(0), \quad \varepsilon - 1 < \gamma \leq \varepsilon. \tag{4}$$

Definition 5. [55]

Let $\mathbb{R}$ be a real set. Then, a fuzzy set $\widetilde{w}$ in $\mathbb{R}$ can be characterized by a membership function $\mu_{\widetilde{w}}$, where, $\mu_{\widetilde{w}}$: $\mathbb{R} \longrightarrow [0,1]$. An $\mathbb{r}$-level set of $\widetilde{w}$ is $[\widetilde{w}]^{\mathbb{r}} = \{w \in \mathbb{R}: \mu_{\widetilde{w}}(w) \geq \mathbb{r}\}$ for $\mathbb{r} \in [0,1]$.

The following are some conditions for a fuzzy set $\widetilde{w}$ to be a fuzzy number:

(i) $\widetilde{w}$ is normal, that is, for $w_0 \in \mathbb{R}$, we have $\mu_{\widetilde{w}}(w_0) = 1$

(ii) $\tilde{w}$ is convex, that is, $\mu_{\tilde{w}}(\nu w_1 + (1-\nu) w_2) \geq \min\{\mu_{\tilde{w}}(w_1), \mu_{\tilde{w}}(w_2)\}$ for all $w_1, w_2 \in \mathbb{R}$ and $\nu \in [0,1]$

(iii) $\tilde{w}$ is semicontinuous

(iv) The set $\overline{\{w \in \mathbb{R}\colon \mu_{\tilde{w}}(w) > 0\}}$ is compact

Definition 6. [56]

A fuzzy number $\tilde{w}$ is classified as a triangular fuzzy number (TFN) if it is defined by three numbers (k_1, k_2, k_3) with $k_1 < k_2 < k_3$ such that it forms a triangle. Its membership function is as follows:

$$\mu(w, k_1, k_2, k_3) = \begin{cases} 0, & w \leq k_1, \\ \dfrac{w - k_1}{k_2 - k_1}, & k_1 \leq w \leq k_2, \\ \dfrac{k_3 - w}{k_3 - k_2}, & k_2 \leq w \leq k_3, \\ 0, & w \geq k3. \end{cases} \tag{5}$$

By utilizing the $\mathbb{r}$-cut notion, the interval form of TFN can be expressed as follows:

$$\tilde{w} = [\underline{w}, \overline{w}] = [k_1 + (k_2 - k_1)\mathbb{r}, k_3 - (k_3 - k_2)\mathbb{r}], \tag{6}$$

where $\underline{w}$ and $\overline{w}$ represent the lower and upper bounds, respectively, for $\mathbb{r} \in [0, 1]$.

Definition 7. [56]

A fuzzy number $\tilde{w}(\mathbb{r})$ can also be represented as $\tilde{w} = [\underline{w}, \overline{w}]$ which satisfies the following conditions:

(i) $\underline{w}(\mathbb{r})$ is a bounded monotonic increasing left continuous function

(ii) $\overline{w}(\mathbb{r})$ is a bounded monotonic decreasing left continuous function

(iii) $\underline{w}(\mathbb{r}) \leq \overline{w}(\mathbb{r})$ for $\mathbb{r} \in [0, 1]$

3. Fuzzy-Fractional Modeling of the Financial Chaotic System

This section is focused on the modeling of the fuzzy-fractional chaotic financial system that is mostly used in the financial and economic sectors. We consider the chaotic financial system given as follows:

$$\begin{aligned} &\frac{\partial \mathcal{G}1}{\partial \tau} - \mathcal{G}3(\tau) - \mathcal{G}2(\tau)\mathcal{G}1(\tau) + \mathbb{A}\mathcal{G}1(\tau) = 0, \\ &\frac{\partial \mathcal{G}2}{\partial \tau} - 1 + \mathbb{B}\mathcal{G}2(\tau) + \mathcal{G}1^2(\tau) = 0, \\ &\frac{\partial \mathcal{G}3}{\partial \tau} + \mathcal{G}1(\tau) + \mathbb{C}\mathcal{G}3(\tau) = 0, \quad \tau > 0, \end{aligned} \tag{7}$$

with conditions

$$\begin{aligned} \mathcal{G}1(0) &= \mathbb{Y}1, \\ \mathcal{G}2(0) &= \mathbb{Y}2, \\ \mathcal{G}3(0) &= \mathbb{Y}3, \end{aligned} \tag{8}$$

where $\mathcal{G}1$, $\mathcal{G}2$, and $\mathcal{G}3$ represent the interest rate, investment demand, and price index, respectively. Moreover, $\mathbb{A}$ denotes the saving amount, $\mathbb{B}$ is the per-investment cost, and the parameter $\mathbb{C}$ presents the elasticity of demands. For a precise understanding of the interest rate, investment demand, and price index, the given system is modeled in fractional form by utilizing Definition 3, which is presented in the following equation:

$$\begin{aligned} &\frac{\partial^{\gamma} \mathcal{G}1}{\partial \tau^{\gamma}} - \mathcal{G}3(\tau) - \mathcal{G}2(\tau)\mathcal{G}1(\tau) + \mathbb{A}\mathcal{G}1(\tau) = 0, \\ &\frac{\partial^{\gamma} \mathcal{G}2}{\partial \tau^{\gamma}} - 1 + \mathbb{B}\mathcal{G}2(\tau) + \mathcal{G}1^2(\tau) = 0, \\ &\frac{\partial^{\gamma} \mathcal{G}3}{\partial \tau^{\gamma}} + \mathcal{G}1(\tau) + \mathbb{C}\mathcal{G}3(\tau) = 0, \quad 0 < \gamma \leq 1, \tau > 0, \end{aligned} \tag{9}$$

where γ represents the fractional parameter in a Caputo sense. To introduce uncertainty in the system, we have incorporated triangular fuzzy numbers in given initial conditions $\mathbb{Y}i$, $i = 1, 2, 3$ by utilizing Definition 5–7. In parametric form, they can be written as $\tilde{\mathbb{Y}}1 = [0 + (0.3 - 0)\mathbb{r}, 1 - (1 - 0.3)\mathbb{r}]$, $\tilde{\mathbb{Y}}2 = [-1 + (-0.3 + 1)\mathbb{r}, 1 - (1 + 0.3)\mathbb{r}]$, and $\tilde{\mathbb{Y}}3 = [0 + (0.2 - 0)\mathbb{r}, 1 - (1 - 0.2)\mathbb{r}]$. Thus, the fuzzy-fractional chaotic financial system is as follows:

$$\begin{aligned} &\frac{\partial^{\gamma} \tilde{\mathcal{G}}1}{\partial \tau^{\gamma}} - \tilde{\mathcal{G}}3(\tau) - \tilde{\mathcal{G}}2(\tau)\tilde{\mathcal{G}}1(\tau) + \mathbb{A}\tilde{\mathcal{G}}1(\tau) = 0, \\ &\frac{\partial^{\gamma} \tilde{\mathcal{G}}2}{\partial \tau^{\gamma}} - 1 + \mathbb{B}\tilde{\mathcal{G}}2(\tau) + \tilde{\mathcal{G}}1^2(\tau) = 0, \\ &\frac{\partial^{\gamma} \tilde{\mathcal{G}}3}{\partial \tau^{\gamma}} + \tilde{\mathcal{G}}1(\tau) + \mathbb{C}\tilde{\mathcal{G}}3(\tau) = 0, \quad 0 < \gamma \leq 1, \tau > 0, \end{aligned} \tag{10}$$

with fuzzy initial conditions

$$\begin{aligned} \tilde{\mathcal{G}}1(0) &= \tilde{\mathbb{Y}}1, \\ \tilde{\mathcal{G}}2(0) &= \tilde{\mathbb{Y}}2, \\ \tilde{\mathcal{G}}3(0) &= \tilde{\mathbb{Y}}3. \end{aligned} \tag{11}$$

The system in (10) along with its fuzzy conditions (11) will be utilized by financial analysts and investors to predict the characteristics of the financial market. It can provide an excellent tool to make informed investment decisions in the areas of financial risk management.

4. Solution Framework Based on the Extended He–Mohand Algorithm for Fuzzy-Fractional Systems

Let us consider a general nonlinear fuzzy-fractional system,

$$\mathbb{D}_{\tau}^{\gamma}\widetilde{\mathscr{G}}j(\tau)+\mathscr{L}[\widetilde{\mathscr{G}}j(\tau)]+\mathscr{N}[\widetilde{\mathscr{G}}j(\tau)]=0,\quad j=1,\ldots,m,\tau>0,\ \varepsilon-1<\gamma\leq\varepsilon, \tag{12}$$

with fuzzified initial conditions

$$\widetilde{\mathscr{G}}j(0)=\mathscr{A}j,\quad j=1,\ldots,m, \tag{13}$$

where γ is the Caputo fractional parameter, $\mathbb{D}_{\tau}^{\gamma}$ is the fractional derivative of $\widetilde{\mathscr{G}}j$, and j represents the total equations of the system. The parameters $\mathscr{L}$ and $\mathscr{N}$ are linear and nonlinear operators, respectively.

Equation (12) can be expressed by using $\mathbb{r}$-cut as follows:

$$\left[\mathbb{D}_{\tau}^{\gamma}\underline{\mathscr{G}}j(\tau;\mathbb{r}),\mathbb{D}_{\tau}^{\gamma}\overline{\mathscr{G}}j(\tau;\mathbb{r})\right]+\left[\mathscr{L}[\underline{\mathscr{G}}j(\tau;\mathbb{r})],\mathscr{L}[\overline{\mathscr{G}}j(\tau;\mathbb{r})]\right]+\left[\mathscr{N}[\underline{\mathscr{G}}j(\tau;\mathbb{r})],\mathscr{N}[\overline{\mathscr{G}}j(\tau;\mathbb{r})]\right]=0, \tag{14}$$

where $\widetilde{\mathscr{G}}j(\tau;\mathbb{r})=[\underline{\mathscr{G}}j(\tau;\mathbb{r}),\overline{\mathscr{G}}j(\tau;\mathbb{r})]$. $\underline{\mathscr{G}}j(\tau;\mathbb{r})$ represents the lower bound solution and $\overline{\mathscr{G}}j(\tau;\mathbb{r})$ represents the upper bound solution.

First, we take Mohand transform on both sides of (12) as follows:

$$\mathscr{M}_{\tau}\left\{\mathbb{D}_{\tau}^{\gamma}\widetilde{\mathscr{G}}j(\tau;\mathbb{r})\right\}+\mathscr{M}_{\tau}\left\{\mathscr{L}[\widetilde{\mathscr{G}}j(\tau;\mathbb{r})]+\mathscr{N}[\widetilde{\mathscr{G}}j(\tau;\mathbb{r})]\right\}=0. \tag{15}$$

Application of Definition 4 gives

$$\mathscr{M}_{\tau}\left\{\widetilde{\mathscr{G}}j(\tau;\mathbb{r})\right\}-\left(\frac{1}{p^{\gamma}}\right)\sum_{a=0}^{\varepsilon-1}p^{\gamma-a+1}\widetilde{\mathscr{G}}j^{(a)}(0)+\left(\frac{1}{p^{\gamma}}\right)\mathscr{M}_{\tau}\left\{\mathscr{L}[\widetilde{\mathscr{G}}j(\tau;\mathbb{r})]+\mathscr{N}[\widetilde{\mathscr{G}}j(\tau;\mathbb{r})]\right\}=0. \tag{16}$$

The general homotopy of the system is as follows:

$$\begin{aligned}\text{Hom: }&(1-q)\left(\mathscr{M}_{\tau}\left\{\widetilde{\mathscr{G}}j(\tau;\mathbb{r})\right\}-\widetilde{\mathscr{G}}j_0\right)+q\Bigg(\mathscr{M}_{\tau}\left\{\widetilde{\mathscr{G}}j(\tau;\mathbb{r})\right\}-\left(\frac{1}{p^{\gamma}}\right)\sum_{a=0}^{\varepsilon-1}p^{\gamma-a+1}\widetilde{\mathscr{G}}j^{(a)}(0)\\&+\left(\frac{1}{p^{\gamma}}\right)\mathscr{M}_{\tau}\left\{\mathscr{L}[\widetilde{\mathscr{G}}j(\tau;\mathbb{r})]+\mathscr{N}[\widetilde{\mathscr{G}}j(\tau;\mathbb{r})]\right\}\Bigg)=0,\end{aligned} \tag{17}$$

with $\widetilde{\mathscr{G}}j_0$ as an initial guess and $q\in[0,1]$. Expansion of $\widetilde{\mathscr{G}}j(\tau;\mathbb{r})$ in power series form w.r.t. q gives

$$\widetilde{\mathscr{G}}j(\tau;\mathbb{r})=\sum_{n=0}^{\infty}q^{n}\widetilde{\mathscr{G}}j_n(\tau;\mathbb{r}). \tag{18}$$

Substituting (18) in (17) and comparing similar coefficients of power of q leads to q^1 where

$$\mathscr{M}_{\tau}\left\{\widetilde{\mathscr{G}}j_1(\tau;\mathbb{r})\right\}+\widetilde{\mathscr{G}}j_0-\left(\frac{1}{p^{\gamma}}\right)\sum_{a=0}^{\varepsilon-1}p^{\gamma-a+1}\widetilde{\mathscr{G}}j^{(a)}(0)+\left(\frac{1}{p^{\gamma}}\right)\mathscr{M}_{\tau}\left\{\mathscr{L}\left[\widetilde{\mathscr{G}}j_0(\tau;\mathbb{r})\right]+\mathscr{N}\left[\widetilde{\mathscr{G}}j_0(\tau;\mathbb{r})\right]\right\}=0. \tag{19}$$

At q^2, we obtain

$$\mathscr{M}_{\tau}\left\{\widetilde{\mathscr{G}}j_2(\tau;\mathbb{r})\right\}+\left(\frac{1}{p^{\gamma}}\right)\mathscr{M}_{\tau}\left\{\mathscr{L}\left[\widetilde{\mathscr{G}}j_1(\tau;\mathbb{r})\right]+\mathscr{N}\left[\widetilde{\mathscr{G}}j_1(\tau;\mathbb{r})\right]\right\}=0. \tag{20}$$

In general at q^n, we have

$$\mathcal{M}_{\tau}\left\{\widetilde{\mathcal{G}}j_n(\tau;\mathbb{r})\right\}+\left(\frac{1}{p^{\gamma}}\right)\mathcal{M}_{\tau}\left\{\mathcal{L}\left[\widetilde{\mathcal{G}}j_{n-1}(\tau;\mathbb{r})\right]+\mathcal{N}\left[\widetilde{\mathcal{G}}j_{n-1}(\tau;\mathbb{r})\right]\right\}=0. \tag{21}$$

Applying the inverse Mohand transform gives the following at q^1:

$$\widetilde{\mathcal{G}}j_1(\tau;\mathbb{r})+\mathcal{M}_{\tau}^{-1}\left\{\widetilde{\mathcal{G}}j_0-\left(\frac{1}{p^{\gamma}}\right)\sum_{a=0}^{\varepsilon-1}p^{\gamma-a+1}\widetilde{\mathcal{G}}j^{(a)}(0)+\left(\frac{1}{s^{\gamma}}\right)\mathcal{M}_{\tau}\left\{\mathcal{L}\left[\widetilde{\mathcal{G}}j_0(\tau;\mathbb{r})\right]+\mathcal{N}\left[\widetilde{\mathcal{G}}j_0(\tau;\mathbb{r})\right]\right\}\right\}=0. \tag{22}$$

At q^2, we have

$$\widetilde{\mathcal{G}}j_2(\tau;\mathbb{r})+\mathcal{M}_{\tau}^{-1}\left\{\left(\frac{1}{p^{\gamma}}\right)\mathcal{M}_{\tau}\left\{\mathcal{L}\left[\widetilde{\mathcal{G}}j_1(\tau;\mathbb{r})\right]+\mathcal{N}\left[\widetilde{\mathcal{G}}j_1(\tau;\mathbb{r})\right]\right\}\right\}=0. \tag{23}$$

At q^n, we obtain

$$\widetilde{\mathcal{G}}j_n(\tau;\mathbb{r})+\mathcal{M}_{\tau}^{-1}\left\{\left(\frac{1}{p^{\gamma}}\right)\mathcal{M}_{\tau}\left\{\mathcal{L}\left[\widetilde{\mathcal{G}}j_{n-1}(\tau;\mathbb{r})\right]+\mathcal{N}\left[\widetilde{\mathcal{G}}j_{n-1}(\tau;\mathbb{r})\right]\right\}\right\}=0. \tag{24}$$

The approximate solution of (12) is obtained by

$$\widetilde{\mathcal{G}}j=\sum_{n=0}^{\infty}\widetilde{\mathcal{G}}j_n(\tau;\mathbb{r}). \tag{25}$$

The residual function can be calculated by substituting (25) in the given system (12) as

$$\mathcal{R}_{\widetilde{\mathcal{G}}j}=\mathbb{D}_{\tau}^{\gamma}\widetilde{\mathcal{G}}j+\mathcal{L}[\widetilde{\mathcal{G}}j]+\mathcal{N}[\widetilde{\mathcal{G}}j]. \tag{26}$$

5. Theoretical Analysis of the Extended He–Mohand Algorithm for Fuzzy-Fractional Systems

Theorem 8. *Convergence*

Given that a Banach space has $\widetilde{\mathcal{G}}j_n(\tau)$ and $\widetilde{\mathcal{G}}j(\tau)$ defined in it for $j=2,\ldots,m$. Then, the obtained approximate solution (25) of a fuzzy-fractional differential system for $\mathbb{S}\in(0,1)$ converges to its exact solution (12).

Proof. Let $\{Cj_n\}$ be the sequence of partial sums of (25). In order to show that Cj_n is a Cauchy sequence in Banach space, let us consider

$$\begin{aligned}\left\|Cj_{n+1}-Cj_n\right\|&=\left\|\widetilde{\mathcal{G}}j_{n+1}\right\|\\&\le\mathbb{S}\left\|\widetilde{\mathcal{G}}j_n\right\|\\&\le\mathbb{S}^2\left\|\widetilde{\mathcal{G}}j_{n-1}\right\|\\&\vdots\\&\le\mathbb{S}^{n+1}\left\|\widetilde{\mathcal{G}}j_0\right\|.\end{aligned} \tag{27}$$

By considering Cj_n and Cj_m as partial sums, for $n\ge m$ and $n,m\in\mathbb{N}$, triangle inequality property provides

$$\begin{aligned}\left\|Cj_n-Cj_m\right\|&=\left\|(Cj_n-Cj_{n-1})+(Cj_{n-1}-Cj_{n-2})\right.\\&\quad\left.+\cdots+(Cj_{m+1}-Cj_m)\right\|\\&\le\left\|Cj_n-Cj_{n-1}\right\|+\left\|Cj_{n-1}-Cj_{n-2}\right\|\\&\quad+\cdots+\left\|Cj_{m+1}-Cj_m\right\|.\end{aligned} \tag{28}$$

Utilizing (27) gives

$$\begin{aligned}\|Cj_n - Cj_m\| &\le \mathbb{S}^n\|\tilde{\mathscr{G}}j_0\| + \mathbb{S}^{n-1}\|\tilde{\mathscr{G}}j_0\| + \cdots + \mathbb{S}^{m+1}\|\tilde{\mathscr{G}}j_0\| \\ &\le \left(\mathbb{S}^n + \mathbb{S}^{n-1} + \cdots + \mathbb{S}^{m+1}\right)\|\tilde{\mathscr{G}}j_0\| \\ &\le \mathbb{S}^{m+1}\left(\mathbb{S}^{n-m-1} + \mathbb{S}^{n-m-2} + \cdots + \mathbb{S} + 1\right)\|\tilde{\mathscr{G}}j_0\| \\ &\le \mathbb{S}^{m+1}\left(\frac{1-\mathbb{S}^{n-m}}{1-\mathbb{S}}\right)\|\tilde{\mathscr{G}}j_0\|.\end{aligned} \tag{29}$$

Since $0 < \mathbb{S} < 1$, therefore, $1 - \mathbb{S}^{n-m} < 1$. Thus, we have

$$\|Cj_n - Cj_m\| \le \frac{\mathbb{S}^{m+1}}{1-\mathbb{S}}\max|\tilde{\mathscr{G}}j_0|. \tag{30}$$

The boundedness of $\tilde{\mathscr{G}}j_0$ implies that

$$\lim_{n,m\longrightarrow\infty}\|Cj_n - Cj_m\| = 0. \tag{31}$$

Hence, we proved that Cj_n is a Cauchy sequence in a Banach space. This leads to the convergence of the given scheme. □

Theorem 9. *Error Estimation*

The solution of the fuzzy-fractional system (12) has maximum absolute truncation error given as follows:

$$\left|\tilde{\mathscr{G}}j - \sum_{h=0}^{m}\tilde{\mathscr{G}}j_h\right| \le \frac{\mathbb{S}^{m+1}}{1-\mathbb{S}}\|\tilde{\mathscr{G}}j_0\|. \tag{32}$$

Proof. From equation (29), we obtain

$$\|\tilde{\mathscr{G}}j - Cj_m\| \le \mathbb{S}^{m+1}\left(\frac{1-\mathbb{S}^{n-m}}{1-\mathbb{S}}\right)\|\tilde{\mathscr{G}}j_0\|, \tag{33}$$

where $0 < \mathbb{S} < 1 \Rightarrow 1 - \mathbb{S}^{n-m} < 1$. Thus, we have

$$\left|\tilde{\mathscr{G}}j - \sum_{b=0}^{m}\tilde{\mathscr{G}}j_b\right| \le \frac{\mathbb{S}^{m+1}}{1-\mathbb{S}}\|\tilde{\mathscr{G}}j_0\|. \tag{34}$$

Hence proved. □

6. Application of the Proposed Methodology to the Fuzzy-Fractional Chaotic Financial System

Let us consider the chaotic financial system modeled in fuzzy-fractional form (see (10)) in Section 3,

$$\begin{aligned}&\frac{\partial^\gamma\tilde{\mathscr{G}}1}{\partial\tau^\gamma} - \tilde{\mathscr{G}}3(\tau) - \tilde{\mathscr{G}}2(\tau)\tilde{\mathscr{G}}1(\tau) + \mathbb{A}\tilde{\mathscr{G}}1(\tau) = 0,\\ &\frac{\partial^\gamma\tilde{\mathscr{G}}2}{\partial\tau^\gamma} - 1 + \mathbb{B}\tilde{\mathscr{G}}2(\tau) + \tilde{\mathscr{G}}1^2(\tau) = 0,\\ &\frac{\partial^\gamma\tilde{\mathscr{G}}3}{\partial\tau^\gamma} + \tilde{\mathscr{G}}1(\tau) + \mathbb{C}\tilde{\mathscr{G}}3(\tau) = 0, \quad 0<\gamma\le 1, \tau>0,\end{aligned} \tag{35}$$

with fuzzified conditions (see (11)).

$$\begin{aligned}\tilde{\mathscr{G}}1(0) &= \tilde{\mathbb{Y}}1,\\ \tilde{\mathscr{G}}2(0) &= \tilde{\mathbb{Y}}2,\\ \tilde{\mathscr{G}}3(0) &= \tilde{\mathbb{Y}}3,\end{aligned} \tag{36}$$

where $\tilde{\mathbb{Y}}1 = [0, 0.3, 1]$, $\tilde{\mathbb{Y}}2 = [-1, -0.3, 1]$, and $\tilde{\mathbb{Y}}3 = [0, 0.2, 1]$ are triangular fuzzy numbers.

Solution 10. Initiating Mohand transform and then using the differential property of Mohand transform (4) gives

$$\begin{aligned}p^\gamma\mathscr{M}_\tau\{\tilde{\mathscr{G}}1(\tau;\mathbb{r})\} - p^{\gamma+1}\tilde{\mathbb{Y}}1 + \mathscr{M}_\tau\{-\tilde{\mathscr{G}}3(\tau;\mathbb{r}) - \tilde{\mathscr{G}}2(\tau;\mathbb{r})\tilde{\mathscr{G}}1(\tau;\mathbb{r}) + \mathbb{A}\tilde{\mathscr{G}}1(\tau;\mathbb{r})\} &= 0,\\ p^\gamma\mathscr{M}_\tau\{\tilde{\mathscr{G}}2(\tau;\mathbb{r})\} - p^{\gamma+1}\tilde{\mathbb{Y}}2 + \mathscr{M}_\tau\{-1 + \mathbb{B}\tilde{\mathscr{G}}2(\tau;\mathbb{r}) + \tilde{\mathscr{G}}1^2(\tau;\mathbb{r})\} &= 0,\\ p^\gamma\mathscr{M}_\tau\{\tilde{\mathscr{G}}3(\tau;\mathbb{r})\} - p^{\gamma+1}\tilde{\mathbb{Y}}3 + \mathscr{M}_\tau\{+\tilde{\mathscr{G}}1(\tau;\mathbb{r}) + \mathbb{C}\tilde{\mathscr{G}}3(\tau;\mathbb{r})\} &= 0.\end{aligned} \tag{37}$$

Homotopies of abovementioned system for $q \in [0,1]$ are as follows:

$$\begin{aligned}&\mathbb{H}1: (1-q)\left(\mathscr{M}_\tau\{\tilde{\mathscr{G}}1(\tau;\mathbb{r})\} - \tilde{\mathscr{G}}1_0\right) + q\left(\mathscr{M}_\tau\{\tilde{\mathscr{G}}1(\tau;\mathbb{r})\} - p\tilde{\mathbb{Y}}1 + \left(\frac{1}{p^\gamma}\right)\mathscr{M}_\tau\{-\tilde{\mathscr{G}}3(\tau;\mathbb{r}) - \tilde{\mathscr{G}}2(\tau;\mathbb{r})\tilde{\mathscr{G}}1(\tau;\mathbb{r}) + \mathbb{A}\tilde{\mathscr{G}}1(\tau;\mathbb{r})\}\right) = 0,\\ &\mathbb{H}2: (1-q)\left(\mathscr{M}_\tau\{\tilde{\mathscr{G}}2(\tau;\mathbb{r})\} - \tilde{\mathscr{G}}2_0\right) + q\left(\mathscr{M}_\tau\{\tilde{\mathscr{G}}2(\tau;\mathbb{r})\} - p\tilde{\mathbb{Y}}2 + \left(\frac{1}{p^\gamma}\right)\mathscr{M}_\tau\{-1 + \mathbb{B}\tilde{\mathscr{G}}2(\tau;\mathbb{r}) + \tilde{\mathscr{G}}1^2(\tau;\mathbb{r})\}\right) = 0,\\ &\mathbb{H}3: (1-q)\left(\mathscr{M}_\tau\{\tilde{\mathscr{G}}3(\tau;\mathbb{r})\} - \tilde{\mathscr{G}}3_0\right) + q\left(\mathscr{M}_\tau\{\tilde{\mathscr{G}}3(\tau;\mathbb{r})\} - p\tilde{\mathbb{Y}}3 + \left(\frac{1}{p^\gamma}\right)\mathscr{M}_\tau\{\tilde{\mathscr{G}}1(\tau;\mathbb{r}) + \mathbb{C}\tilde{\mathscr{G}}3(\tau;\mathbb{r})\}\right) = 0.\end{aligned} \tag{38}$$

Substitution of (18) in (38) gives the following at q^1:

$$\begin{aligned}
&\mathcal{M}_\tau\left\{\widetilde{\mathcal{G}}1_1(\tau;\mathbb{r})\right\} + \widetilde{\mathcal{G}}1_0 - p\widetilde{\mathbb{Y}}1 + \left(\frac{1}{p^\gamma}\right)\mathcal{M}_\tau\left\{-\widetilde{\mathcal{G}}3_0(\tau;\mathbb{r}) - \widetilde{\mathcal{G}}2_0(\tau;\mathbb{r})\widetilde{\mathcal{G}}1_0(\tau;\mathbb{r}) + \mathbb{A}\widetilde{\mathcal{G}}1_0(\tau;\mathbb{r})\right\} = 0,\\
&\mathcal{M}_\tau\left\{\widetilde{\mathcal{G}}2_1(\tau;\mathbb{r})\right\} + \widetilde{\mathcal{G}}2_0 - p\widetilde{\mathbb{Y}}2 + \left(\frac{1}{p^\gamma}\right)\mathcal{M}_\tau\left\{-1 + \mathbb{B}\widetilde{\mathcal{G}}2_0(\tau;\mathbb{r}) + \widetilde{\mathcal{G}}1_0^2(\tau;\mathbb{r})\right\} = 0,\\
&\mathcal{M}_\tau\left\{\widetilde{\mathcal{G}}3_1(\tau;\mathbb{r})\right\} + \widetilde{\mathcal{G}}3_0 - p\widetilde{\mathbb{Y}}3 + \left(\frac{1}{p^\gamma}\right)\mathcal{M}_\tau\left\{\widetilde{\mathcal{G}}1_0(\tau;\mathbb{r}) + \mathbb{C}\widetilde{\mathcal{G}}3_0(\tau;\mathbb{r})\right\} = 0.
\end{aligned}\tag{39}$$

Applying the inverse Mohand transform results in

$$\begin{aligned}
\widetilde{\mathcal{G}}1_1(\tau;\mathbb{r}) &= -\frac{(\mathbb{A}\widetilde{\mathbb{Y}}1 - \widetilde{\mathbb{Y}}2\widetilde{\mathbb{Y}}1 - \widetilde{\mathbb{Y}}3)\tau^\gamma}{\Gamma(\gamma+1)},\\
\widetilde{\mathcal{G}}2_1(\tau;\mathbb{r}) &= -\frac{\left(\mathbb{B}\widetilde{\mathbb{Y}}2 + \widetilde{\mathbb{Y}}1^2 - 1\right)\tau^\gamma}{\Gamma(\gamma+1)},\\
\widetilde{\mathcal{G}}3_1(\tau;\mathbb{r}) &= -\frac{(\mathbb{C}\widetilde{\mathbb{Y}}3 + \widetilde{\mathbb{Y}}1)\tau^\gamma}{\Gamma(\gamma+1)}.
\end{aligned}\tag{40}$$

At q^2, we obtain

$$\begin{aligned}
&\mathcal{M}_\tau\left\{\widetilde{\mathcal{G}}1_2(\tau;\mathbb{r})\right\} + \left(\frac{1}{p^\gamma}\right)\mathcal{M}_\tau\left\{-\widetilde{\mathcal{G}}3_1(\tau;\mathbb{r}) - \widetilde{\mathcal{G}}2_1(\tau;\mathbb{r})\widetilde{\mathcal{G}}1_1(\tau;\mathbb{r}) + \mathbb{A}\widetilde{\mathcal{G}}1_1(\tau;\mathbb{r})\right\} = 0,\\
&\mathcal{M}_\tau\left\{\widetilde{\mathcal{G}}2_2(\tau;\mathbb{r})\right\} + \left(\frac{1}{p^\gamma}\right)\mathcal{M}_\tau\left\{-1 + \mathbb{B}\widetilde{\mathcal{G}}2_1(\tau;\mathbb{r}) + \widetilde{\mathcal{G}}1_1^2(\tau;\mathbb{r})\right\} = 0,\\
&\mathcal{M}_\tau\left\{\widetilde{\mathcal{G}}3_2(\tau;\mathbb{r})\right\} + \left(\frac{1}{p^\gamma}\right)\mathcal{M}_\tau\left\{\widetilde{\mathcal{G}}1_1(\tau;\mathbb{r}) + \mathbb{C}\widetilde{\mathcal{G}}3_1(\tau;\mathbb{r})\right\} = 0.
\end{aligned}\tag{41}$$

Applying the inverse Mohand transform gives

$$\begin{aligned}
\widetilde{\mathcal{G}}1_2(\tau;\mathbb{r}) &= \frac{-\tau^{2\gamma}\left(-\widetilde{\mathbb{Y}}1\left(\mathbb{A}^2 - \widetilde{\mathbb{Y}}2(2\mathbb{A}+\mathbb{B}) + \widetilde{\mathbb{Y}}2^2\right) + \widetilde{\mathbb{Y}}3(\mathbb{A}+\mathbb{C}-\widetilde{\mathbb{Y}}2) + \widetilde{\mathbb{Y}}1^3\right)}{\Gamma(2\gamma+1)},\\
\widetilde{\mathcal{G}}2_2(\tau;\mathbb{r}) &= \frac{\tau^{2\gamma}\left(\widetilde{\mathbb{Y}}1^2(2\mathbb{A}+\mathbb{B}-2\widetilde{\mathbb{Y}}2) + \mathbb{B}(\mathbb{B}\widetilde{\mathbb{Y}}2 - 1) - 2\widetilde{\mathbb{Y}}3\widetilde{\mathbb{Y}}1\right)}{\Gamma(2\gamma+1)},\\
\widetilde{\mathcal{G}}3_2(\tau;\mathbb{r}) &= \frac{\tau^{2\gamma}\left(\widetilde{\mathbb{Y}}1(\mathbb{A}+\mathbb{C}-\widetilde{\mathbb{Y}}2) + \left(\mathbb{C}^2 - 1\right)\widetilde{\mathbb{Y}}3\right)}{\Gamma(2\gamma+1)}.
\end{aligned}\tag{42}$$

At q^3, we obtain

$$\begin{aligned}
&\mathscr{M}_{\tau}\left\{\widetilde{\mathscr{G}}1_{3}(\tau;\mathbb{r})\right\}+\left(\frac{1}{p^{\gamma}}\right)\mathscr{M}_{\tau}\left\{-\widetilde{\mathscr{G}}3_{2}(\tau;\mathbb{r})-\widetilde{\mathscr{G}}2_{2}(\tau;\mathbb{r})\widetilde{\mathscr{G}}1_{2}(\tau;\mathbb{r})+\mathbb{A}\widetilde{\mathscr{G}}1_{2}(\tau;\mathbb{r})\right\}=0,\\
&\mathscr{M}_{\tau}\left\{\widetilde{\mathscr{G}}2_{3}(\tau;\mathbb{r})\right\}+\left(\frac{1}{p^{\gamma}}\right)\mathscr{M}_{\tau}\left\{-1+\mathbb{B}\widetilde{\mathscr{G}}2_{2}(\tau;\mathbb{r})+\widetilde{\mathscr{G}}1_{2}^{2}(\tau;\mathbb{r})\right\}=0,\\
&\mathscr{M}_{\tau}\left\{\widetilde{\mathscr{G}}3_{3}(\tau;\mathbb{r})\right\}+\left(\frac{1}{p^{\gamma}}\right)\mathscr{M}_{\tau}\left\{\widetilde{\mathscr{G}}1_{2}(\tau;\mathbb{r})+\mathbb{C}\widetilde{\mathscr{G}}3_{2}(\tau;\mathbb{r})\right\}=0.
\end{aligned}\tag{43}$$

Applying the inverse Mohand transform leads to

$$\begin{aligned}
\widetilde{\mathscr{G}}1_{3}(\tau;\mathbb{r})&=\frac{1}{\Gamma(\gamma+1)^{2}\Gamma(3\gamma+1)}\tau^{3\gamma}-\widetilde{\mathbb{Y}}3\Big(\big(\mathbb{A}^{2}+\mathbb{A}\mathbb{C}+\mathbb{C}^{2}-1\big)\Gamma(\gamma+1)^{2}-\widetilde{\mathbb{Y}}2\big((2\mathbb{A}+\mathbb{C})\Gamma(\gamma+1)^{2}+\mathbb{B}\Gamma(2\gamma+1)\big)\\
&\quad+\Gamma(2\gamma+1)+\widetilde{\mathbb{Y}}2^{2}\Gamma(\gamma+1)^{2}\Big)\\
&\quad+\widetilde{\mathbb{Y}}1\Big(\Gamma(\gamma+1)^{2}\big(\mathbb{A}^{3}-\mathbb{A}+\mathbb{B}-\mathbb{C}\big)\Big)\\
&\quad-\widetilde{\mathbb{Y}}2\Big(\big(3\mathbb{A}^{2}+\mathbb{A}\mathbb{B}+\mathbb{B}^{2}-1\big)\Gamma(\gamma+1)^{2}+(\mathbb{A}\mathbb{B}+1)\Gamma(2\gamma+1)\Big)\\
&\quad+\mathbb{A}\Gamma(2\gamma+1)+\widetilde{\mathbb{Y}}2^{2}\big((3\mathbb{A}+\mathbb{B})\Gamma(\gamma+1)^{2}+\mathbb{B}\Gamma(2\gamma+1)\big)+\widetilde{\mathbb{Y}}2^{3}\big(-\Gamma(\gamma+1)^{2}\big)\\
&\quad-\widetilde{\mathbb{Y}}1^{3}\Big(\mathbb{A}\Gamma(2\gamma+1)+(3\mathbb{A}+\mathbb{B})\Gamma(\gamma+1)^{2}-\widetilde{\mathbb{Y}}2\big(3\Gamma(\gamma+1)^{2}+\Gamma(2\gamma+1)\big)\Big)\\
&\quad+\widetilde{\mathbb{Y}}3\widetilde{\mathbb{Y}}1^{2}\big(2\Gamma(\gamma+1)^{2}+\Gamma(2\gamma+1)\big),\\
\widetilde{\mathscr{G}}2_{3}(\tau;\mathbb{r})&=\frac{-1}{\Gamma(\gamma+1)^{2}\Gamma(3\gamma+1)}\tau^{3\gamma}\widetilde{\mathbb{Y}}1^{2}\Big(\mathbb{A}^{2}\Gamma(2\gamma+1)+\big(2\mathbb{A}^{2}+2\mathbb{A}\mathbb{B}+\mathbb{B}^{2}\big)\Gamma(\gamma+1)^{2}\Big)\\
&\quad-\widetilde{\mathbb{Y}}2\big(\mathbb{A}\Gamma(2\gamma+1)+2(\mathbb{A}+\mathbb{B})\Gamma(\gamma+1)^{2}\big)+\widetilde{\mathbb{Y}}2^{2}\big(2\Gamma(\gamma+1)^{2}+\Gamma(2\gamma+1)\big)\\
&\quad-2\widetilde{\mathbb{Y}}3\widetilde{\mathbb{Y}}1\Big(\mathbb{A}\Gamma(2\gamma+1)+\Gamma(\gamma+1)^{2}(\mathbb{A}+\mathbb{B}+\mathbb{C})-\widetilde{\mathbb{Y}}2\big(\Gamma(\gamma+1)^{2}+\Gamma(2\gamma+1)\big)\Big)\\
&\quad+\mathbb{B}^{3}\widetilde{\mathbb{Y}}2\Gamma(\gamma+1)^{2}-\mathbb{B}^{2}\Gamma(\gamma+1)^{2}-2\widetilde{\mathbb{Y}}1^{4}\Gamma\big((\gamma+1)^{2}+\widetilde{\mathbb{Y}}3^{2}\Gamma(2\gamma+1)\big),\\
\widetilde{\mathscr{G}}3_{3}(\tau;\mathbb{r})&=\frac{-1}{\Gamma(3\gamma+1)}\tau^{3\gamma}\Big(\widetilde{\mathbb{Y}}1\big(\mathbb{A}^{2}-\widetilde{\mathbb{Y}}2(2\mathbb{A}+\mathbb{B}+\mathbb{C})+\mathbb{A}\mathbb{C}+\mathbb{C}^{2}+\widetilde{\mathbb{Y}}2^{2}\big)+\widetilde{\mathbb{Y}}3\big(-\mathbb{A}+\mathbb{C}^{3}-2\mathbb{C}+\widetilde{\mathbb{Y}}2\big)-\widetilde{\mathbb{Y}}1^{3}\Big).
\end{aligned}\tag{44}$$

The higher-order problems and solutions can be calculated in a similar way. Thus, by adding the terms we can get the required approximate solution. The residual error of system (35) can be observed through (26).

7. Results and Discussion

The main objective of the current study is the solution and analysis of a fuzzy-fractional chaotic financial model that depends upon interest rate, price index, and investment demand. It is a highly nonlinear differential system with a time-fractional derivative. The fuzziness in initial conditions $\widetilde{\mathbb{Y}}1$, $\widetilde{\mathbb{Y}}2$, and $\widetilde{\mathbb{Y}}3$ are incorporated with the help of triangular fuzzy numbers (TFNs). The approximate series solution is calculated for both the upper bound and lower bound of TFNs through the He–Mohand technique. In this method, the homotopy perturbation method and Mohand transform are combined to tackle the noninteger order derivative and fuzziness. At different values of time, solution and absolute errors are determined. The accuracy of the proposed methodology can be seen from absolute residual and system errors (Tables 1 and 2) that range from 10^{-6} to 10^{-12} at the upper bound and from 10^{-6} to 10^{-11} at the lower bound for fractional parameter $\gamma = 0.89$ and 1.0 and $\mathbb{r} = 0.8$.

To analyze the behavior of interest rate, investment demand, and price index across the fuzzy domain, three-dimensional plots are created. From Figure 1, it can be observed that in the case of lower bound solutions, increasing the value of $\mathbb{r}$-cut decreases the rate of interest, investment demand, and price index. On the other hand, the

Table 1: Upper and lower bound solutions and errors at $\mathbb{A} = \mathbb{B} = \mathbb{C} = 0.01$, $\mathbb{r} = 0.8$, and $\gamma = 0.89$.

	τ	Solution			Absolute errors			
		$\widetilde{\mathscr{G}}1$	$\widetilde{\mathscr{G}}2$	$\widetilde{\mathscr{G}}3$	$\lvert\mathscr{R}\rvert_{\widetilde{\mathscr{G}}1}$	$\lvert\mathscr{R}\rvert_{\widetilde{\mathscr{G}}2}$	$\lvert\mathscr{R}\rvert_{\widetilde{\mathscr{G}}3}$	$\lvert\mathscr{R}\rvert_{\widetilde{\mathscr{G}}-\text{system}}$
$\overline{\mathscr{G}}(\tau;\mathbb{r})$	0.1	0.246633	−0.313071	0.127044	1.28×10^{-8}	1.74×10^{-10}	6.07×10^{-9}	6.35×10^{-9}
	0.2	0.251791	−0.205296	0.098220	4.90×10^{-7}	3.20×10^{-10}	2.46×10^{-7}	2.45×10^{-7}
	0.3	0.256299	−0.103982	0.070471	4.04×10^{-6}	5.89×10^{-8}	2.14×10^{-6}	2.08×10^{-6}
	0.4	0.260353	−0.006756	0.043282	1.77×10^{-5}	5.08×10^{-7}	9.97×10^{-6}	9.41×10^{-6}
	0.5	0.264054	0.087470	0.016437	5.51×10^{-5}	2.37×10^{-6}	3.28×10^{-5}	3.01×10^{-5}
$\underline{\mathscr{G}}(\tau;\mathbb{r})$	0.1	0.484377	0.065320	0.297071	5.15×10^{-8}	1.83×10^{-8}	1.24×10^{-8}	2.74×10^{-8}
	0.2	0.520534	0.150092	0.238334	2.07×10^{-6}	6.96×10^{-7}	5.03×10^{-7}	1.09×10^{-6}
	0.3	0.553101	0.225697	0.178841	1.79×10^{-5}	5.73×10^{-6}	4.39×10^{-6}	9.35×10^{-6}
	0.4	0.582844	0.294436	0.118016	8.27×10^{-5}	2.54×10^{-5}	2.04×10^{-5}	4.28×10^{-5}
	0.5	0.609988	0.357481	0.055758	2.69×10^{-4}	8.02×10^{-5}	6.71×10^{-5}	1.39×10^{-4}

Table 2: Upper and lower bound solutions and errors at $\mathbb{A} = \mathbb{B} = \mathbb{C} = 0.01$, $\mathbb{r} = 0.8$, and $\gamma = 1.0$.

	τ	Solution			Absolute errors			
		$\widetilde{\mathscr{G}}1$	$\widetilde{\mathscr{G}}2$	$\widetilde{\mathscr{G}}3$	$\lvert\mathscr{R}\rvert_{\widetilde{\mathscr{G}}1}$	$\lvert\mathscr{R}\rvert_{\widetilde{\mathscr{G}}2}$	$\lvert\mathscr{R}\rvert_{\widetilde{\mathscr{G}}3}$	$\lvert\mathscr{R}\rvert_{\widetilde{\mathscr{G}}-\text{system}}$
$\overline{\mathscr{G}}(\tau;\mathbb{r})$	0.1	0.245020	−0.345490	0.135598	6.78×10^{-11}	8.22×10^{-12}	2.54×10^{-11}	3.38×10^{-11}
	0.2	0.249716	−0.251312	0.110736	8.35×10^{-9}	9.35×10^{-10}	3.26×10^{-9}	4.18×10^{-9}
	0.3	0.254131	−0.157456	0.085443	1.37×10^{-7}	1.41×10^{-8}	5.57×10^{-8}	6.90×10^{-8}
	0.4	0.258305	−0.063910	0.059746	9.86×10^{-7}	9.25×10^{-8}	4.17×10^{-7}	4.98×10^{-7}
	0.5	0.262273	0.029330	0.033669	4.50×10^{-6}	3.82×10^{-7}	1.99×10^{-6}	2.29×10^{-6}
$\underline{\mathscr{G}}(\tau;\mathbb{r})$	0.1	0.473284	0.039131	0.313990	5.06×10^{-11}	1.29×10^{-10}	8.29×10^{-11}	8.77×10^{-11}
	0.2	0.505566	0.115083	0.264750	5.78×10^{-9}	1.50×10^{-8}	1.06×10^{-8}	1.04×10^{-8}
	0.3	0.536854	0.187749	0.212381	8.75×10^{-8}	2.30×10^{-7}	1.81×10^{-7}	1.66×10^{-7}
	0.4	0.567106	0.257040	0.156990	2.74×10^{-7}	1.54×10^{-6}	1.35×10^{-6}	1.15×10^{-6}
	0.5	0.596234	0.322897	0.098685	2.36×10^{-6}	6.46×10^{-6}	6.47×10^{-6}	5.10×10^{-6}

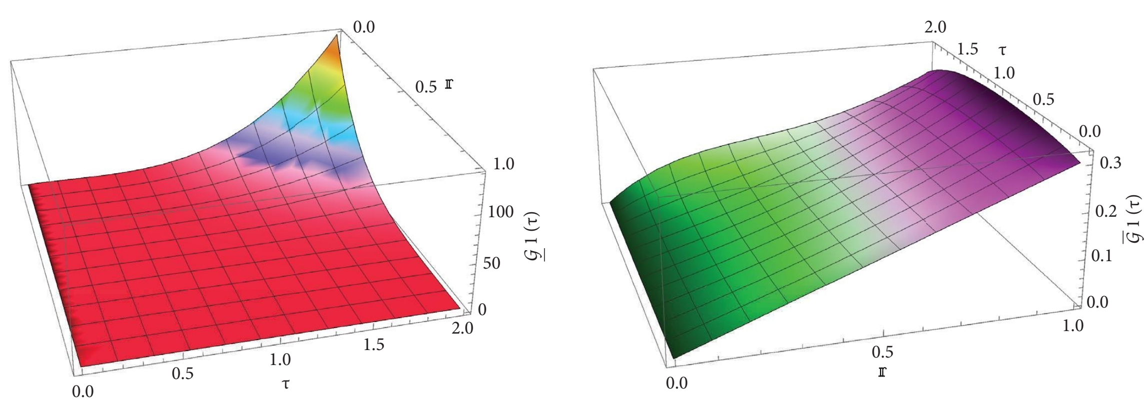

(a)

(b)

Figure 1: Continued.

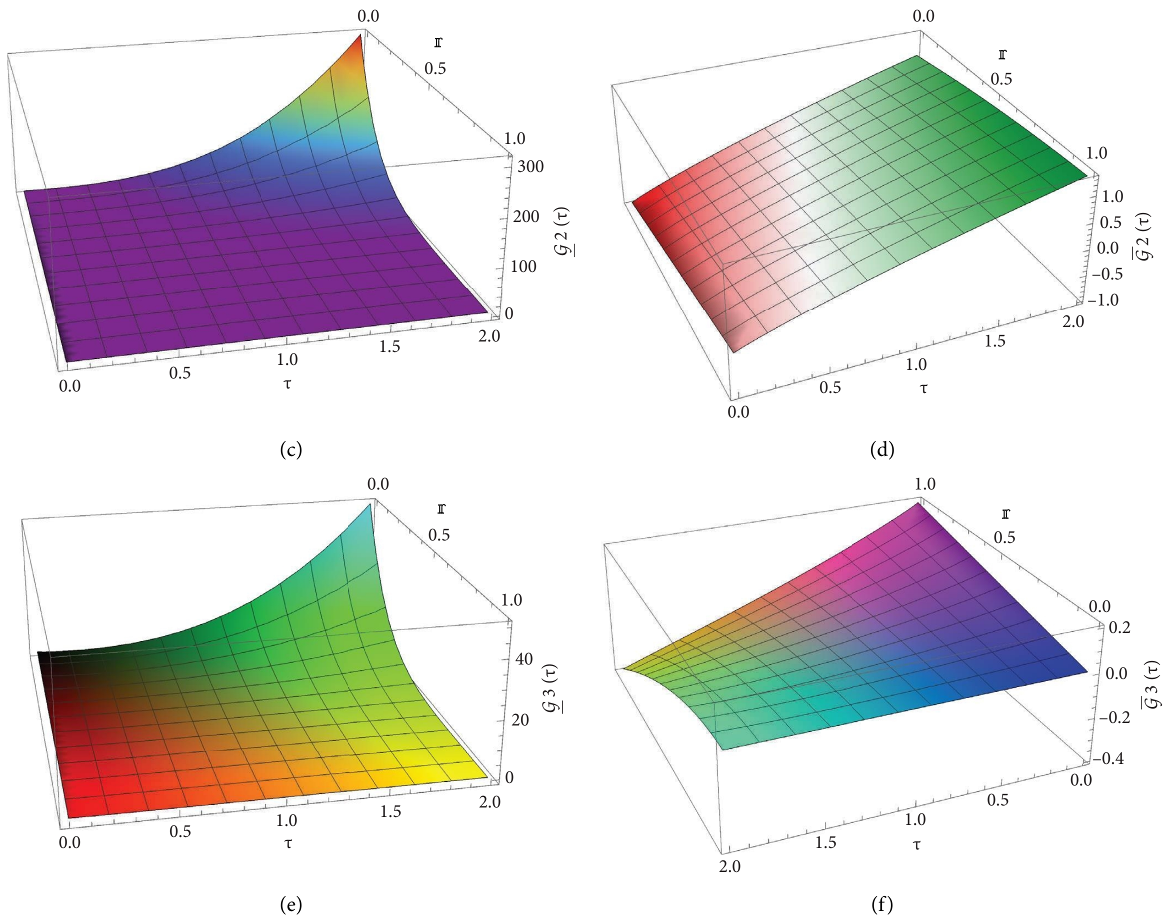

Figure 1: 3D fuzzy upper and lower bound solutions at $\mathbb{A} = 0.20$, $\mathbb{B} = 0.10$, $\mathbb{C} = 0.11$, and $\gamma = 0.51$.

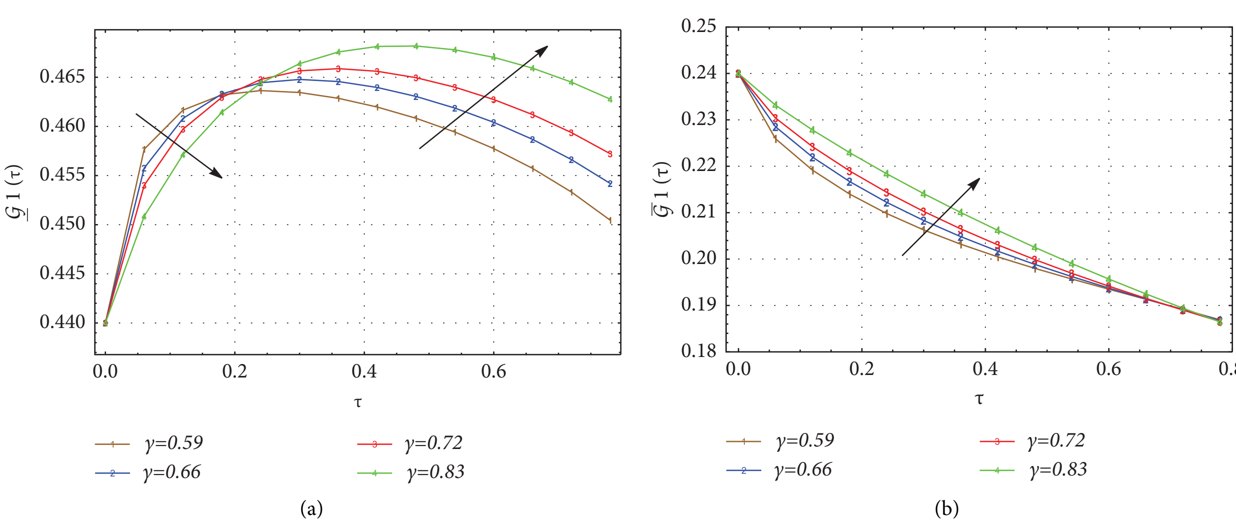

Figure 2: Continued.

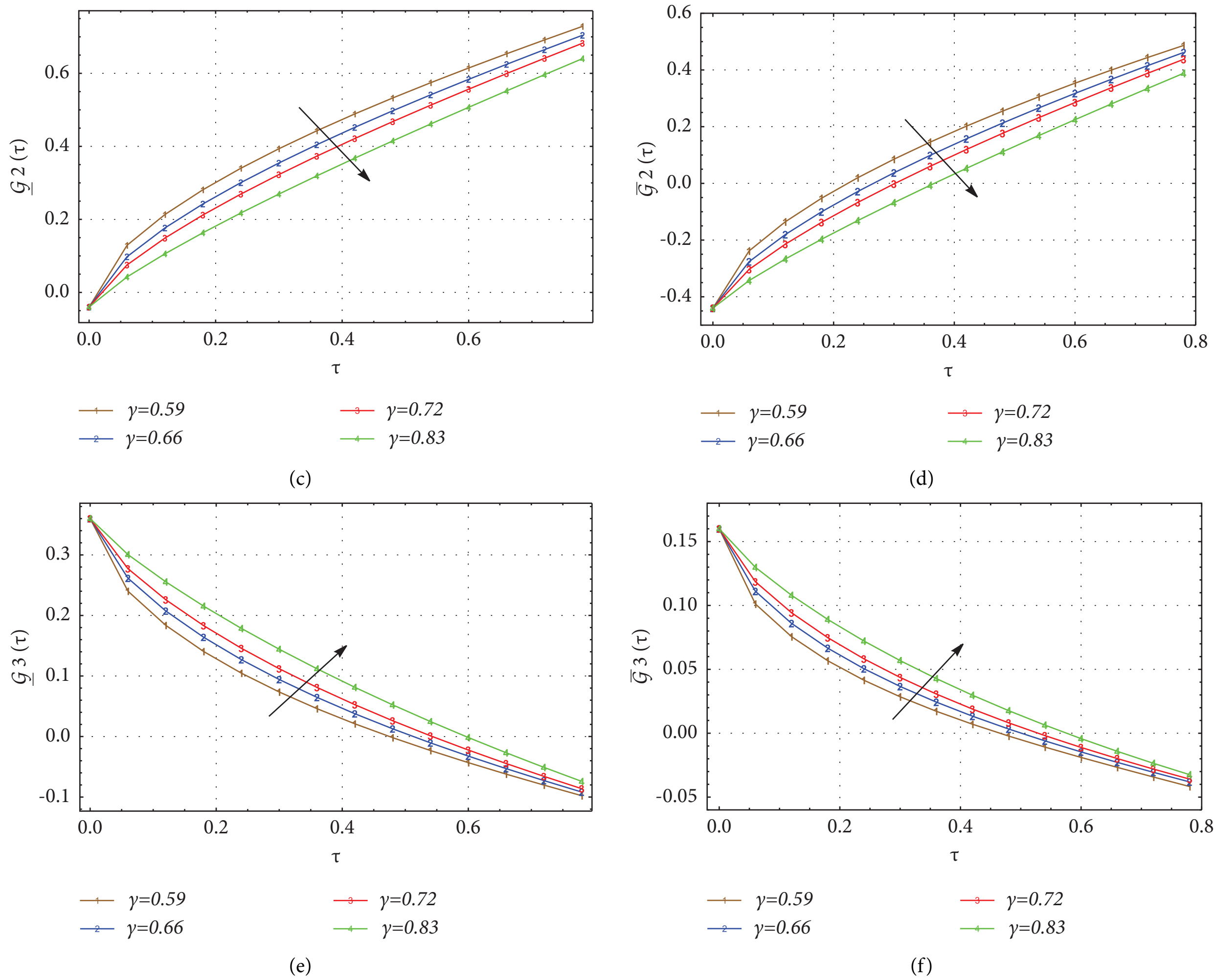

FIGURE 2: 2D fuzzy upper and lower bound solutions at different fractional order γ when $\mathbb{A} = 0.5$, $\mathbb{B} = 0$, $\mathbb{C} = 0.4$, and $\mathbb{r} = 0.8$.

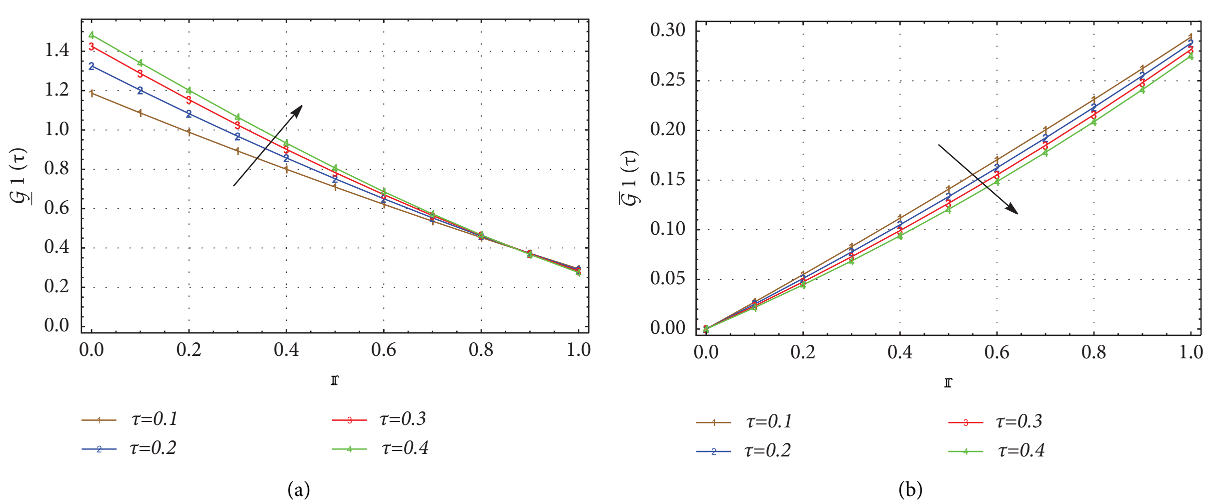

FIGURE 3: Continued.

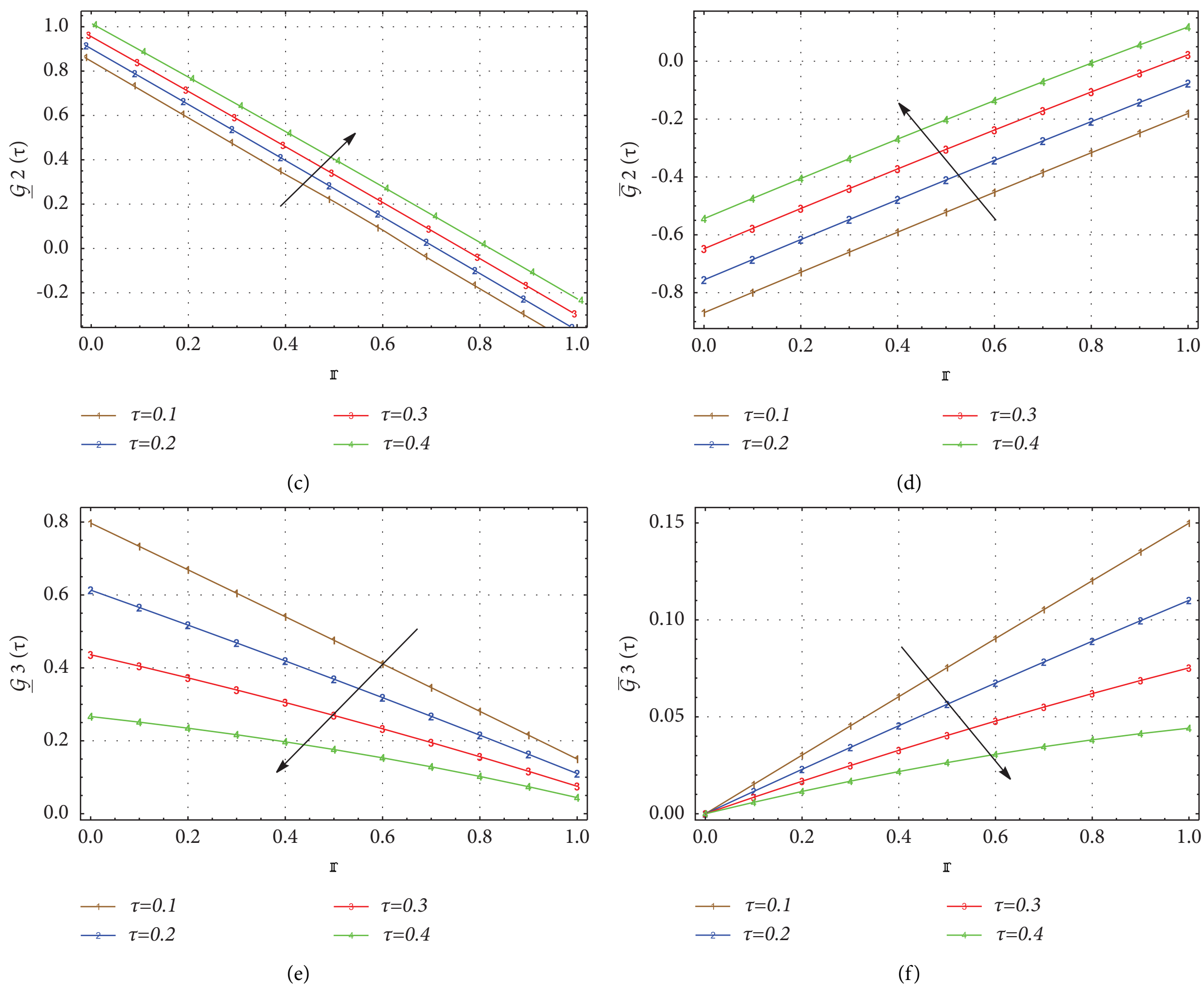

FIGURE 3: 2D fuzzy upper and lower bound solutions at varying values of time τ when $\mathbb{A} = 0.5$, $\mathbb{B} = 0.0$, $\mathbb{C} = 0.5$, and $\gamma = 0.9$.

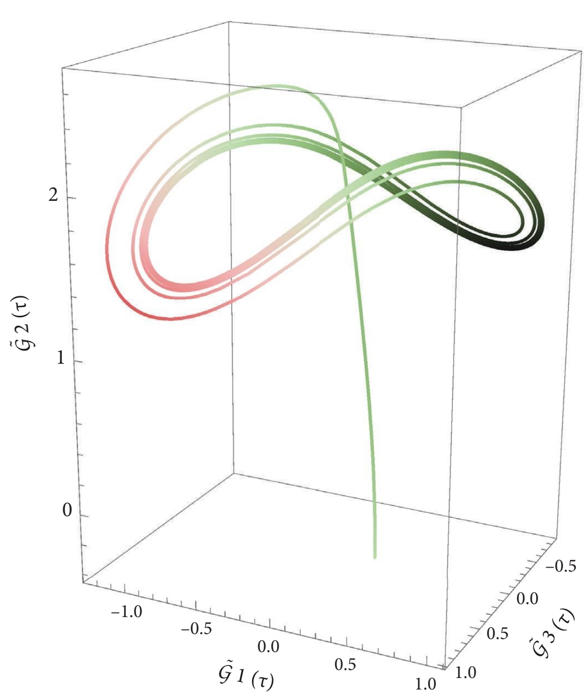

FIGURE 4: Dynamic behavior of interest rate, investment demand, and price index at $\mathbb{A} = 1.1$, $\mathbb{B} = 0.33$, $\mathbb{C} = 0.97$, $\gamma = 0.95$, and $\mathbb{r} = 1$.

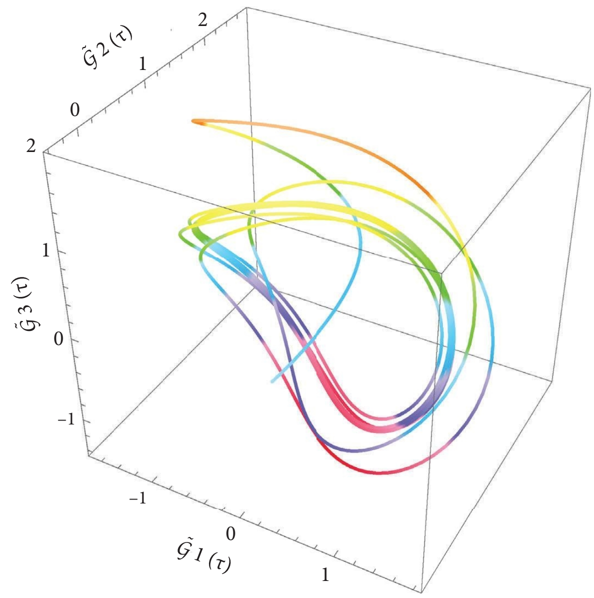

Figure 5: Dynamic behavior of interest rate, investment demand, and price index at $\mathbb{A} = 0.9$, $\mathbb{B} = 0.2$, $\mathbb{C} = 0.3$, $\gamma = 0.95$, and $\mathbb{r} = 1$.

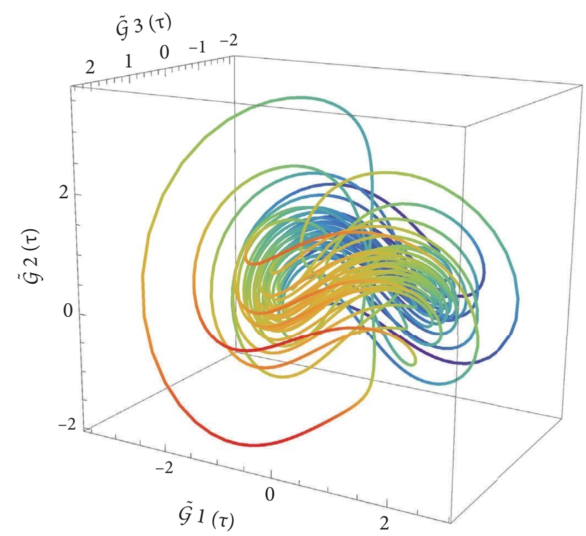

Figure 6: Dynamic behavior of interest rate, investment demand, and price index at $\mathbb{A} = 0.43$, $\mathbb{B} = 0.0$, $\mathbb{C} = 0.12$, $\gamma = 0.95$, and $\mathbb{r} = 1$.

rate of interest, investment demand, and price index increase with the increase in $\mathbb{r}$-cut value. At $\mathbb{r} = 0$, the given fuzzy-fractional chaotic system shows maximum uncertainty. The fuzziness in interest rate, investment demand, and price index begins to decline when $\mathbb{r}$ expands in its domain as they eventually convert to their crisp form at $\mathbb{r} = 1$. Figure 2 illustrates the impact of various fractional parameter values with time on the profiles of interest rate, investment demand, and price index in two-dimensional formation. It is seen that at the lower bound solution of interest rate, initially, the solution profile decreases before changing course after a certain time. In the case of an upper bound, the fractional parameter exhibits a rise in the interest rate. The upper and lower bound profile of the chaotic system increases along with the fractional parameter for the price index. However, the investment demand declines with an increment in the fractional parameter value.

In Figure 3, the behavior of interest rate, investment demand, and price index is demonstrated across the fuzzy domain for different values of the time. It is displayed through arrows that the interest rate at the lower bound rises as time increases. On the other hand, it is declining in the case of the upper bound. At both the upper and lower bounds, overtime the investment demand shows a rise while the price index depreciates. Furthermore, the chaotic patterns of the system at different values of saving amount, per-investment cost, and elasticity in demands with respect to interest rate, investment demand, and price index are illustrated in Figures 4–6 at $\gamma = 1$ and fractional parameter $\gamma = 0.97$. A significant increase in the chaotic behavior of interest rate, investment demand, and price index is observed as the value of saving rate, elasticity of demands, and per-investment cost decreases.

8. Conclusion

The purpose of this research article is the modeling and analysis of the fuzzy-fractional financial chaotic model. Here, we combine fuzzy logic with fractional calculus through an efficient semianalytical methodology which is known as the He–Mohand algorithm. The time-fractional derivative in the model is considered in the Caputo sense. The triangular fuzzy numbers (TFNs) approach is used to include the uncertainty in the system. Error analysis spanning across the $\mathbb{r}$-cut domain is illustrated through tables. It is seen that the obtained errors range from 10^{-6} to 10^{-12} at the upper bound and from 10^{-6} to 10^{-11} at the lower bound. The efficiency of the proposed methodology is also presented in the theoretical analysis. From this, it can be noticed that the He–Mohand algorithm is a convergent scheme. The behavior of interest rate, investment demand, and price index is analyzed in two-dimensional and three-dimensional plots at both upper and lower bounds. The effect of time and fractional parameters on the system profile with regard to $\mathbb{r}$-cut is also studied. It is estimated that as $\mathbb{r}$-cut approaches to 1, correspondingly solution becomes less fuzzy and eventually changes into a crisp form at $\mathbb{r} = 1$. It is also observed that the smaller value saving rate, elasticity of demands, and per-investment cost has a significant effect on the chaotic behavior of the system. In conclusion, the modeled fuzzy-fractional financial chaotic system has the potential in helping the analyst to better comprehend the predictions and risk assessments of financial systems. Moreover, the proposed methodology can be efficiently utilized to tackle various research areas of the financial market such as risk analysis, portfolio administration, and decision-making procedures in fractional and fuzzy environments in the future.

Data Availability

The data used to support the findings of this study are included within the article.

Conflicts of Interest

The authors declare that they have no conflicts of interest.

References

[1] B. Simon, *Financial Modeling*, MIT press, Cambridge, MA, USA, 2014.

[2] C. Z. Mooney, *Monte Carlo Simulation*, Sage, Thousand Oaks, CA, USA, 1997.

[3] W. J. Dixon and F. J. Massey, *Introduction to Statistical Analysis*, Springer, Berlin, Germany, 1951.

[4] A. Saltelli, "Sensitivity analysis for importance assessment," *Risk Analysis*, vol. 22, no. 3, pp. 579–590, 2002.

[5] L. Kruschwitz and A. Löffler, *Discounted Cash Flow: A Theory of the Valuation of Firms*, John Wiley & Sons, Hoboken, NJ, USA, 2006.

[6] E. Parzen, "An approach to time series analysis," *The Annals of Mathematical Statistics*, vol. 32, no. 4, pp. 951–989, 1961.

[7] N. R. Draper and H. Smith, *Applied Regression Analysis*, vol. 326, John Wiley & Sons, Hoboken, NJ, USA, 1998.

[8] L. Liang and X. Cai, "Time-sequencing european options and pricing with deep learning – analyzing based on interpretable ALE method," *Expert Systems with Applications*, vol. 187, Article ID 115951, 2022.

[9] J.-P. Oosterom and C. A. S. Hall, "Enhancing the evaluation of energy investments by supplementing traditional discounted cash flow with energy return on investment analysis," *Energy Policy*, vol. 168, Article ID 112953, 2022.

[10] M. Qayyum, E. Ahmad, S. T. Saeed, A. Akgül, and S. M. El Din, "New solutions of fractional 4d chaotic financial model with optimal control via he-laplace algorithm," *Ain Shams Engineering Journal*, Article ID 102503, 2023.

[11] B. Li, X. Li, K. L. Teo, and P. Zheng, "A new uncertain random portfolio optimization model for complex systems with downside risks and diversification," *Chaos, Solitons and Fractals*, vol. 160, Article ID 112213, 2022.

[12] M. Tian, H. Li, J. Huang, J. Liang, W. Bu, and B. Chen, "Credit risk models using rule-based methods and machine-learning algorithms," in *Proceedings of the 2022 6th International Conference on Computer Science and Artificial Intelligence*, ACM, Beijing China, December, 2022.

[13] L. A. Zadeh, "Fuzzy sets," *Information and Control*, vol. 8, no. 3, pp. 338–353, 1965.

[14] M. Nadeem, I. Siddique, R. Ali et al., "Study of third-grade fluid under the fuzzy environment with Couette and Poiseuille flows," *Mathematical Problems in Engineering*, vol. 2022, Article ID 2458253, 19 pages, 2022.

[15] V. Bobkov, V. Borisov, and Y. Fedulov, "Hybrid fuzzy kinetic model of phosphorite pellets drying process," *Journal of Physics: Conference Series*, vol. 1553, no. 1, Article ID 012014, 2020.

[16] X. Peng and H. Huang, "Fuzzy decision making method based ON COCOSO with critic for financial risk evaluation," *Technological and Economic Development of Economy*, vol. 26, no. 4, pp. 695–724, 2020.

[17] L. Jing, Y. Zhan, Q. Li et al., "An integrated product conceptual scheme decision approach based on shapley value method and fuzzy logic for economic-technical objectives trade-off under uncertainty," *Computers and Industrial Engineering*, vol. 156, Article ID 107281, 2021.

[18] S. Das, S. K. Mahato, and P. Mahato, "Biological control of infection pervasive via pest: a study of prey–predator model incorporating prey refuge under fuzzy impreciseness," *International Journal of Modelling and Simulation*, vol. 42, no. 4, pp. 628–652, 2021.

[19] G. Gumah, S. Al-Omari, and D. Baleanu, "Soft computing technique for a system of fuzzy volterra integro-differential equations in a hilbert space," *Applied Numerical Mathematics*, vol. 152, pp. 310–322, 2020.

[20] M. Qayyum, A. Tahir, S. T. Saeed, and A. Akgül, "Series-form solutions of generalized fractional-Fisher models with uncertainties using hybrid approach in caputo sense," *Chaos, Solitons and Fractals*, vol. 172, Article ID 113502, 2023.

[21] F. S. Pedro, L. C. de Barros, and E. Esmi, "Population growth model via interactive fuzzy differential equation," *Information Sciences*, vol. 481, pp. 160–173, 2019.

[22] Y. Shen, "First-order linear fuzzy differential equations on the space of linearly correlated fuzzy numbers," *Fuzzy Sets and Systems*, vol. 429, pp. 136–168, 2022.

[23] S. Moi, S. Biswas, and S. P. Sarkar, "Finite-difference method for fuzzy singular integro-differential equation deriving from fuzzy non-linear differential equation," *Granular Computing*, vol. 8, no. 3, pp. 503–524, 2022.

[24] P. L. Butzer and U. Westphal, "AN introduction to fractional calculus," in *Applications of Fractional Calculus in Physics*, pp. 1–85, World Scientific, Singapore, 2000.

[25] S. Kumar, R. Kumar, R. P. Agarwal, and B. Samet, "A study of fractional lotka-volterra population model using haar wavelet and adams-bashforth-moulton methods," *Mathematical Methods in the Applied Sciences*, vol. 43, no. 8, pp. 5564–5578, 2020.

[26] M. Qayyum, E. Ahmad, H. Ahmad, and B. Almohsen, "New solutions of time-space fractional coupled Schrödinger systems," *AIMS Mathematics*, vol. 8, no. 11, pp. 27033–27051, 2023.

[27] Farnaz, M. Qayyum, S. I. A. Shah, S. W. Yao, N. Imran, and M. Sohail, "Homotopic fractional analysis of thin film flow of Oldroyd 6-constant fluid," *Alexandria Engineering Journal*, vol. 60, no. 6, pp. 5311–5322, 2021.

[28] X. Ma, M. Xie, W. Wu, B. Zeng, Y. Wang, and X. Wu, "The novel fractional discrete multivariate grey system model and its applications," *Applied Mathematical Modelling*, vol. 70, pp. 402–424, 2019.

[29] B. Ghanbari, S. Kumar, and R. Kumar, "A study of behaviour for immune and tumor cells in immunogenetic tumour model with non-singular fractional derivative," *Chaos, Solitons and Fractals*, vol. 133, Article ID 109619, 2020.

[30] M. Qayyum, E. Ahmad, S. Tauseef Saeed, H. Ahmad, and S. Askar, "Homotopy perturbation method-based soliton solutions of the time-fractional (2+1)-dimensional Wu–zhang system describing long dispersive gravity water waves in the ocean," *Frontiers in Physics*, vol. 11, jun 2023.

[31] S. Rashid, R. Ashraf, and Z. Hammouch, "New generalized fuzzy transform computations for solving fractional partial differential equations arising in oceanography," *Journal of Ocean Engineering and Science*, vol. 8, no. 1, pp. 55–78, 2023.

[32] R. Alyusof, S. Alyusof, N. Iqbal, and S. K. Samura, "Novel evaluation of fuzzy fractional biological population model," *Journal of Function Spaces*, vol. 2022, Article ID 4355938, 9 pages, 2022.

[33] P. Verma, M. Kumar, and A. Shukla, "Analysis on krasnoselskii's fixed point theorem of fuzzy variable fractional

differential equation for a novel coronavirus (COVID-19) model with singular operator," *International Journal of Modeling, Simulation, and Scientific Computing*, vol. 12, no. 03, Article ID 2150034, 2021.

[34] M. Arfan, K. Shah, T. Abdeljawad, and Z. Hammouch, "An efficient tool for solving two-dimensional fuzzy fractional-ordered heat equation," *Numerical Methods for Partial Differential Equations*, vol. 37, no. 2, pp. 1407–1418, 2020.

[35] M. Qayyum, A. Tahir, and S. Acharya, "New solutions of fuzzy-fractional Fisher models via optimal he–laplace algorithm," *International Journal of Intelligent Systems*, vol. 2023, Article ID 7084316, 21 pages, 2023.

[36] M. Caputo, "Mean fractional-order-derivatives differential equations and filters," *Annali dell'Universita di Ferrara*, vol. 41, no. 1, pp. 73–84, 1995.

[37] A. Haq, "Partial-approximate controllability of semi-linear systems involving two riemann-liouville fractional derivatives," *Chaos, Solitons and Fractals*, vol. 157, Article ID 111923, apr 2022.

[38] N. Sene, "Analytical investigations of the fractional free convection flow of brinkman type fluid described by the caputo fractional derivative," *Results in Physics*, vol. 37, Article ID 105555, jun 2022.

[39] M. Qayyum, E. Ahmad, M. B. Riaz, J. Awrejcewicz, and S. T. Saeed, "New soliton solutions of time-fractional korteweg–de vries systems," *Universe*, vol. 8, no. 9, p. 444, 2022.

[40] M. Vellappandi, P. Kumar, V. Govindaraj, and W. Albalawi, "An optimal control problem for mosaic disease via caputo fractional derivative," *Alexandria Engineering Journal*, vol. 61, no. 10, pp. 8027–8037, 2022.

[41] P. Sunthrayuth, N. H. Aljahdaly, A. Ali, R. Shah, I. Mahariq, and A. M. J. Tchalla, "Φ-Haar Wavelet Operational Matrix Method for Fractional Relaxation-Oscillation Equations Containing Φ-Caputo Fractional Derivative," *Journal of function spaces*, vol. 2021, Article ID 7117064, 14 pages, 2021.

[42] P. Kumar, D. Baleanu, V. S. Erturk, M. Inc, and V. Govindaraj, "A delayed plant disease model with caputo fractional derivatives," *Advances in Continuous and Discrete Models*, vol. 2022, no. 1, 2022.

[43] M. Qayyum, S. Afzal, E. Ahmad, and M. B. Riaz, "Fractional modeling and analysis of unsteady squeezing flow of casson nanofluid via extended he-laplace algorithm in liouville-caputo sense," *Alexandria Engineering Journal*, vol. 73, pp. 579–591, 2023.

[44] N. Sene, "Analysis of a fractional-order chaotic system in the context of the caputo fractional derivative via bifurcation and lyapunov exponents," *Journal of King Saud University Science*, vol. 33, no. 1, Article ID 101275, 2021.

[45] V. Rexma Sherine, P. Chellamani, R. Ismail, N. Avinash, and G. Britto Antony Xavier, "Estimating the spread of generalized compartmental model of monkeypox virus using a fuzzy fractional laplace transform method," *Symmetry*, vol. 14, no. 12, p. 2545, 2022.

[46] N. Najafi and T. Allahviranloo, "Combining fractional differential transform method and reproducing kernel hilbert space method to solve fuzzy impulsive fractional differential equations," *Computational and Applied Mathematics*, vol. 39, no. 2, p. 122, 2020.

[47] A. A. Alderremy, J. F. Gómez-Aguilar, S. Aly, and K. M. Saad, "A fuzzy fractional model of coronavirus (COVID-19) and its study with legendre spectral method," *Results in Physics*, vol. 21, Article ID 103773, 2021.

[48] Z. Alijani, D. Baleanu, B. Shiri, and G.-C. Wu, "Spline collocation methods for systems of fuzzy fractional differential equations," *Chaos, Solitons and Fractals*, vol. 131, Article ID 109510, 2020.

[49] M. Alaroud, M. Al-Smadi, R. Rozita Ahmad, and U. K. Salma Din, "An analytical numerical method for solving fuzzy fractional volterra integro-differential equations," *Symmetry*, vol. 11, no. 2, p. 205, 2019.

[50] S. Kumar, J. J. Nieto, and B. Ahmad, "Chebyshev spectral method for solving fuzzy fractional fredholm–volterra integro-differential equation," *Mathematics and Computers in Simulation*, vol. 192, pp. 501–513, 2022.

[51] Y. Liu, Y. Zhang, and J. Pang, "Approximate solutions to shallow water wave equations by the homotopy perturbation method coupled with mohand transform," *Frontiers in Physics*, vol. 10, 2023.

[52] M. Mohand and A. Mahgoub, "The new integral transform "mohand transform"," *Advances in Theoretical and Applied Mathematics*, vol. 12, no. 2, pp. 113–120, 2017.

[53] V. S. Erturk, A. Ahmadkhanlu, P. Kumar, and V. Govindaraj, "Some novel mathematical analysis on a corneal shape model by using caputo fractional derivative," *Optik*, vol. 261, Article ID 169086, 2022.

[54] M. Nadeem, Z. Li, and Y. Alsayyad, "Analytical approach for the approximate solution of harry dym equation with caputo fractional derivative," *Mathematical Problems in Engineering*, vol. 2022, Article ID 4360735, 7 pages, 2022.

[55] D. Qiu, C. Lu, W. Zhang, Q. Zhang, and C. Mu, "Basic theorems for fuzzy differential equations in the quotient space of fuzzy numbers," *Advances in Difference Equations*, vol. 2014, no. 1, 2014.

[56] S. Sindu Devi and K. Ganesan, "Application of linear fuzzy differential equation in day to day life," in *AIP Conference Proceedings*, AIP Publishing, New York, NY, USA, 2019.